A SHORT NOTE ON PERMEABILITY ANISOTROPY IN HETEROGENEOUS POROUS MEDIA

by

Xiaomin Zhao and M. Nafi Toksöz

Earth Resources Laboratory
Department of Earth, Atmospheric, and Planetary Sciences
Massachusetts Institute of Technology
Cambridge, MA 02139

ABSTRACT

This paper presents some new results of theoretical modeling on permeability anisotropy in heterogeneous porous media. It is shown that the lineation of heterogeneities results in permeability anisotropy. However, to produce strong anisotropy, the permeability contrast between the lineated high permeability region and the background must be very high. We demonstrate this using two examples. The first is the fracture model in which the background has negligible permeability compared to the fractures. In the second example the fractures are replaced by impermeable stripes and the background has high permeability. In both cases permeability anisotropy with an order of magnitude difference is produced. These results compare well with the results of laboratory experiments performed to evaluate permeability anisotropy.

INTRODUCTION

Permeability anisotropy is of interest in the study of fluid flow in reservoirs. Recent studies have emerged in this research area (Gibson and Toksöz, 1990; Bernabé, 1991; Zhao and Toksöz, 1991). These studies demonstrated that the condition for producing strong permeability anisotropy is that the permeability contrast between the lineated permeable region and the less permeable region should be large, as in the lineated fracture case (Zhao and Toksöz, 1991). In this study, we show that strong anisotropy can also result from the case where the medium contains some impermeable layers sandwiched between permeable regions. The modeling techniques were described in Zhao and Toksöz (1991). A Successive Over-Relaxation (SOR) finite-difference scheme was used to simulate the fluid flow field, and the lineated Gaussian correlation function was used to produce the lineated heterogeneities.

Bernabé (1991) performed a set of permeability measurements on synthetic anisotropic

samples. These results provide experimental evidence of permeability anisotropy. Two sets of experimental results are of particular interest to this study. In one case permeable layers are sandwiched between less-permeable porous plates. But the permeability contrast between the two types of regions is not very large. In the second case, thin layers with very low permeability are sandwiched between the permeable layers and the porous plates. The two data sets will be modeled using the finite-difference algorithm. The data sets, coupled with theoretical results, demonstrate that the permeability contrast is the key factor controlling the degree of anisotropy.

MODELING EXAMPLES

(1) Lineated Heterogeneities (Low Permeability Contrast)

The effects of lineated heterogeneities have been studied by Zhao and Toksöz (1991). Here we present the results of the theoretical modeling in order to explain the experimental results of Bernabé (1991), which will be described later. The heterogeneous distributions are generated using different correlation lengths in the Gaussian correlation function ($a_1 = 20$ and $a_2 = 2$, respectively, see Zhao and Toksöz, 1991). The flow fields have been calculated for various θ values between 0° and 90°. As an example, the aligned medium and the simulated flow field at $\theta = 45°$ are given in Figure 1. Because of the lineation of permeability heterogeneities, the flow tends to channel through high permeability regions. This is shown clearly in Figure 1b, where the lineation of high and low permeability strips makes the flow field have a trend to deflect toward the lineation of high permeability regions. Figure 2 shows the calculated average flow versus θ. The permeability is the maximum along $\theta = 0°$, and becomes minimum along $\theta = 90°$; the anisotropy (defined as $(k_0 - k_{90})/((k_0 + k_{90})/2)$) for this case is about 10%. By varying the correlation lengths a_1 and a_2, the degree of anisotropy does not significantly exceed this value due to the random medium model used here. In this model, a region with moderate and low permeabilities is sandwiched between two adjacent high permeability regions. Therefore flow can always cross the less permeable region without having to flow around the region. Thus due to the presence of background permeability, the lineation of random heterogeneities cannot result in anisotropic permeabilities that are an order of magnitude difference. In order to produce a strong permeability anisotropy, the permeability contrast between the permeable stripes and the background must be high. This will be the case of fractures studied in the following section.

(2) Fracture Model I (Permeable Channels – Impermeable Background)

Since fractures can contribute significantly to the reservoir permeability, it is important to model the effects of fracture permeability. As shown by Gibson and Toksöz (1990),

a primary effect of fracture is anisotropy in permeability. Because of the alignment of fractures, the permeability can vary with orientation by orders of magnitude. The major features of fracture fluid flow are that the background has negligible permeability and that the flow is highly concentrated along the fractures. This situation can be modeled using the random medium model as follows. We choose the aspect ratio, $a_1/a_2 \gg 1$, so that the heterogeneities are highly lineated. In order to remove the background permeability, we set a threshold, say, 60% of the maximum $[\alpha(x,y)]$. The values of $\alpha(x,y)$ that are smaller than this threshold are set to a very small number; values greater than the threshold are kept unchanged. Figures 3a and 3c show the $\alpha(x,y)$ distributions that resemble a natural fracture network. The permeability contrast between the fracture and the background is 600:1. Although the background permeability may still be large compared to typical fractured rocks (granite, limestone, etc.), the highly conductive channels (fractures) conduct most of the flow so that the background flow is small. In this way the flow in the fracture network is simulated. The calculated flow field along and perpendicular to the fracture alignment is shown in Figures 3b and 3d. The flow patterns for the two orientations are quite different. As expected, the flow is highly channeled along the fractures. For the $\theta = 90^o$ case (Figure 3d) the flow has to wind around the junctions of the fractures, while in the $\theta = 0°$ case flow takes place along the straight channel. These result in significant permeability difference for the two cases. We have performed the calculation for various orientations. Figure 4 shows the calculated average flow as a function of the orientation θ. In this figure, the permeability is maximum along fractures and minimum perpendicular to them, the same as in the previous case of aligned heterogeneities. However, the permeability difference between $\theta = 0°$ and $\theta = 90°$ is 184% in the present case.

(3) Fracture Model II (Impermeable Barriers – Permeable Background)

The above fracture model shows that strong permeability anisotropy exists in lineated heterogeneous porous media only when the permeability contrast between the permeable channels (fractures) and the less permeable background is large. It is interesting to study the case where the background becomes permeable while the flow channels (fractures) are sealed (impermeable). This model can be generated from the previous lineated heterogeneity model, in the same way as the above fracture model. We set a threshold, say, 40% of the maximum permeability value of the model. The regions whose permeability is less than this threshold is assigned to a very small value (about 1/600 of the maximum permeability). Figures 5a, c, and e show heterogeneity models for the angle of lineation $\theta = 0^o$, 45°, and 90° cases, together with the simulated flow field, Figures 5b, d, f. Because of the no-flow barriers in the heterogeneous distribution, the flow has to wind around these barriers. For the $\theta = 0^o$ case, the flow takes place along the lineation of the barriers, while for the $\theta = 90^o$ case, the flow has to penetrate the junctions between the barriers and the flow paths are longer than in the $\theta = 0^o$ case.

Therefore, flow fields along and perpendicular to the channels are very different. This results in significant permeability anisotropy. Figure 6 shows the calculated average flow as a function of the angle of lineation θ. The permeability difference between $\theta = 0^o$ and $\theta = 90^o$ is about 175%, almost the same order as the previous fracture model.

COMPARISON WITH EXPERIMENTAL DATA MEASURED FROM MATERIALS WITH ANISOTROPIC PERMEABILITY

In a recently published paper Bernabé (1991) showed the experimental results of permeability measurements on anisotropic materials. These experiments were performed to evaluate the validity of the tensor form of Darcy's law in anisotropic porous media. In that study a 2-D finite-difference simulation using the anisotropic tensor form Darcy's law was also performed. Excellent agreement was found between the numerical analysis and the experiment. The experimental results provide a test of the present numerical analysis of heterogeneous media.

The experiments were performed on anisotropic porous medium samples made from a stack of identical flat porous plates. In the sample, the space between two adjacent plates was deliberately left open. It was hoped that these openings would act as high permeability channels, analogous to fractures. However, it turned out that the ratio of permeabilities measured perpendicular and parallel to the plates was only about 0.6, the material obtained being only moderately anisotropic. In fact, these experimental results are quite consistent with our modeling results for the aligned permeability distribution (Figure 1), which shows that the lineation of high permeability channels (analogous to the openings between the plates) surrounded by a less permeable background (analogous to the synthetic porous plates) cannot result in significant permeability anisotropy.

As described in Bernabé's (1991) paper, in order to provide a highly anisotropic permeability model, a large percentage of the top surface of each plate was coated with a thin layer of impermeable silicone rubber so that the flow perpendicular to the plates was largely reduced. This time a permeability ratio of 0.02 for $\theta = 0°$ and $90°$ was obtained. To determine the variation of permeability measured along different directions, the synthetic materials of both cases (i.e., permeability ratios of 0.6 and of 0.02) were cut at $0°$, $15°$, $30°$, and $45°$ with respect to the direction parallel to the plates. Permeabilities along these directions were measured, with other sides of the (cubic) sample that are parallel to the measurement direction sealed with a jacket (no flow boundaries). The experimental results are replotted here in Figure 7 (crosses). The anisotropic finite-difference modeling results of Bernabé (1991) are also represented in the same figure (triangles). It is seen that strong permeability anisotropy is produced by the impermeable layer, with the ratio of permeabilities measured perpendicular and parallel to the plates being 0.02. This result is also consistent with the modeling results for the permeable background with impermeable barriers (Figure 6). We model the

experimental results quantitatively using our finite-difference formulation and show that a macroscopically anisotropic permeability medium can result from a microscopically isotropic but heterogeneous medium.

Figure 8 shows our finite-difference model composed of stacked plates. The permeability of the plates and that of the opening are denoted by k_p and k_0, respectively. A thin region with permeability k_c is used to model the less permeable layer due to the silicone rubber coating. The three permeabilities are determined as follows. In the first, we determined k_p and k_0 in the absence of the k_c region. Given the measured permeabilities at $\theta = 0°$ and $\theta = 90°$, k_p and k_0 can be uniquely determined. For the model shown in Figure 8, $k_p = 1$ Darcy and $k_0 = 0.1$ Darcy. This is the case with the permeability ratio equal to 0.6. In the second step, the k_c region is introduced between k_p and k_0 regions and the value of k_c is adjusted to obtain the measured permeability ratio of 0.02 for $\theta = 90°$ and $0°$. This value is found to be 4×10^{-4} Darcy. From the model of Figure 8, square models were cut at $\theta = 0°$, $15°$, $30°$, $45°$, $60°$, $75°$, and $90°$ with respect to the direction parallel to the plates. Each model includes 16 plates. For the models with given θ values, finite-difference modeling was carried out and the average permeability for each θ was calculated. The results are given in Figure 10 (circles), together with the experimental results and those from the anisotropic finite-difference modeling (Bernabé, 1991). Clearly, the results from our finite-difference modeling agree well with both results. The agreement with experimental results verifies for the validity of our heterogeneous finite difference formulation. More important, the agreement with Bernabé's (1991) anisotropic finite difference results indicates that the permeability anisotropy on a macroscopic scale can result from heterogeneities composed of microscopically isotropic materials.

CONCLUSIONS

The purpose of this study was to demonstrate that permeability contrast between permeable and impermeable regions in lineated heterogeneous porous media is the key factor controlling the degree of permeability anisotropy. Strong anisotropy exists only when the contrast is large. This implies that strong anisotropy will exist in reservoirs consisting of lineated fractures or in reservoirs containing nonpermeable barriers, such as the sand-shale sequence commonly encountered in reservoirs.

ACKNOWLEDGEMENTS

86ER13636.

REFERENCES

Bernabé, Y.,1991, On the measurement of permeability in anisotropic rocks. *Fault Mechanism and Transport Properties of Rocks: A Festchrift in Honor of W. F. Brace*, B. Evans and T. F. Wong (eds), Academic Press, London, in press.

Gibson, R.L., Jr. and M.N. Toksöz, 1990, Permeability estimation from velocity anisotropy in fractured rock, *J. Geophys. Res., 95*, 15643–15655.

Zhao, X.M. and M.N. Toksöz, 1991, Permeability anisotropy in heterogeneous porous media, *SEG Abstracts, D/P1.7*, 387–390.
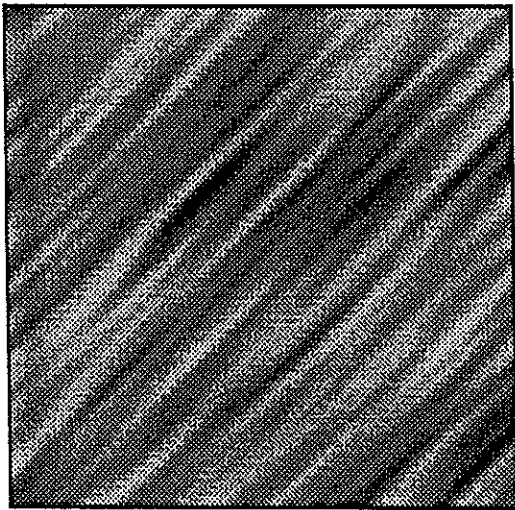
(a)
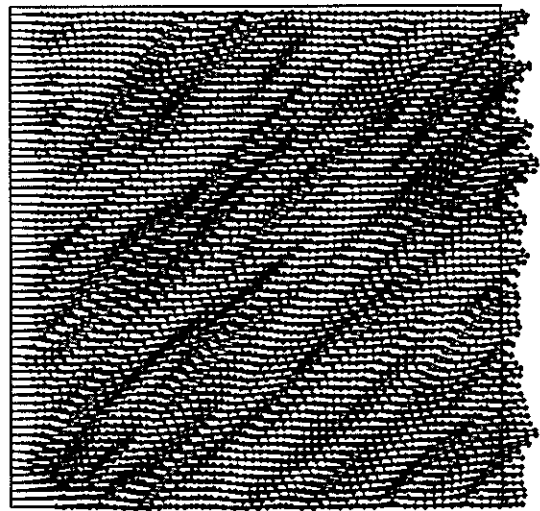
(b)

Figure 1: (a): Aligned distribution with $\theta = 45°$ calculated using Gaussian correlation functions. The two correlation lengths are $a_1 = 20$, $a_2 = 2$. Model lengths are $x_0 = y_0 = 128$.

(b): calculated flow fields.
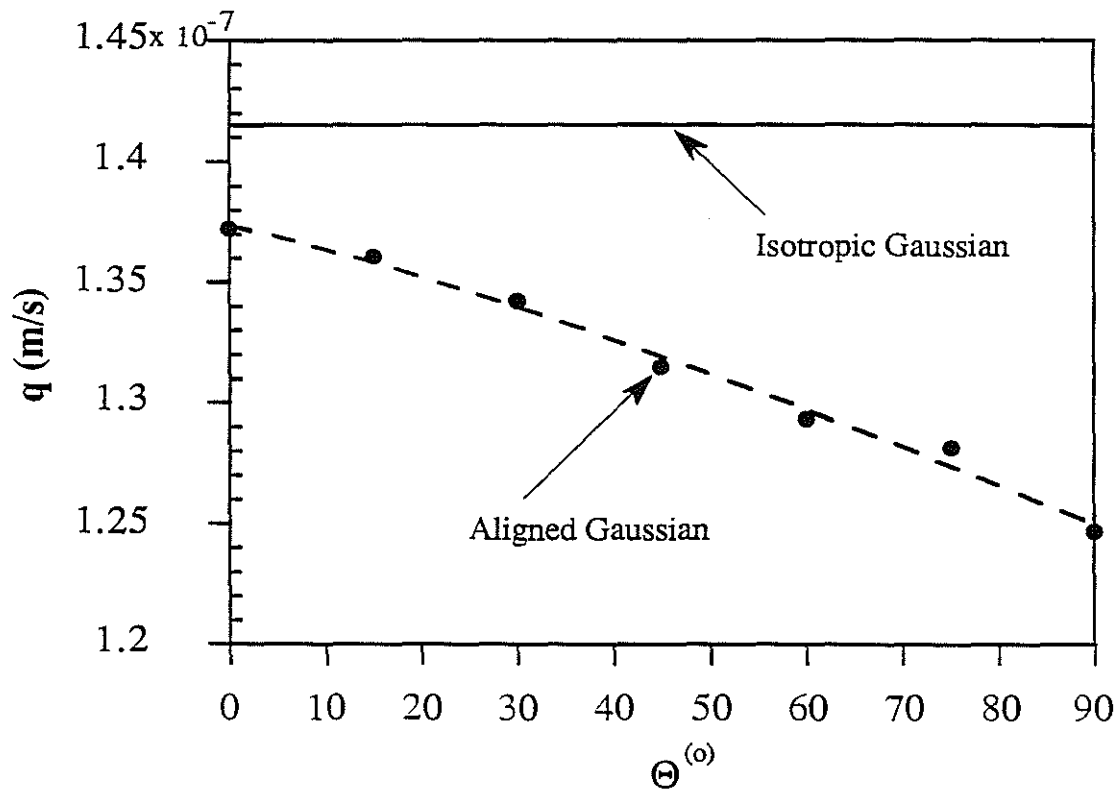
Figure 2: Average flow $\bar{q}$ versus angle of alignment for the cases of aligned distributions. The case of isotropic Gaussian ($a = 20$) is also plotted for comparison (solid line). Although permeability anisotropy is present, its magnitude is only about 10%.
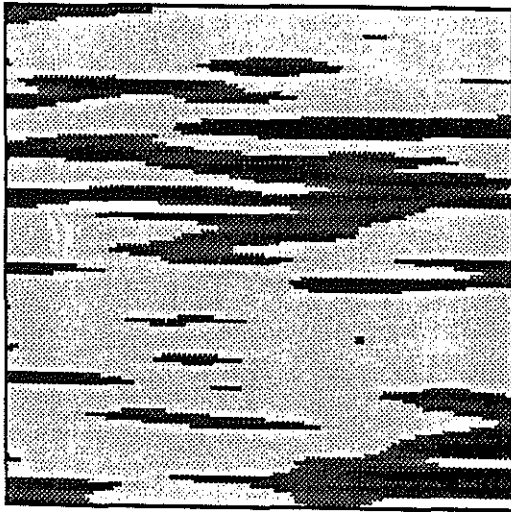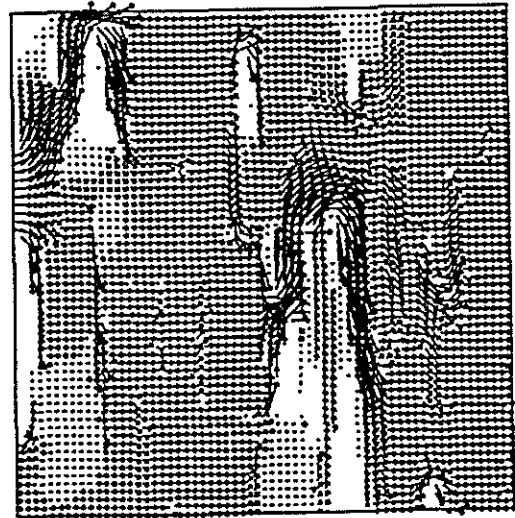
(a)
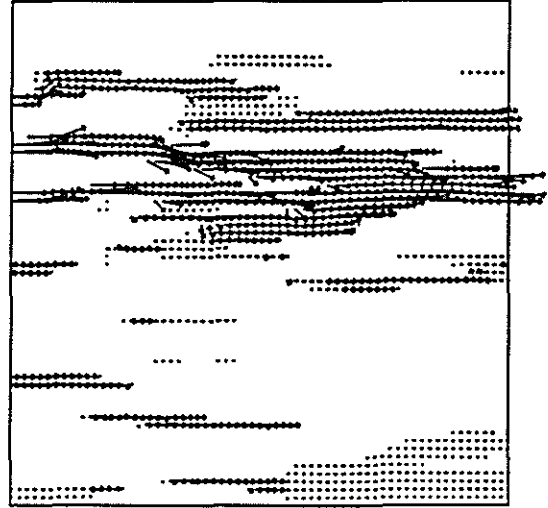
(b)
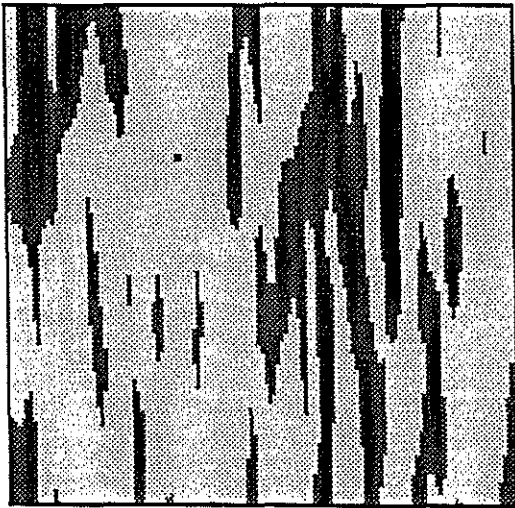
(c)

(d)

Figure 3: (a) and (c): Aligned fracture distributions with $\theta = 0°$ (a) and $90°$ (c). The correlation lengths and model lengths are the same as in Figure 4. (b) and (d): calculated flow for $\theta = 0°$ (b) and $90°$ (d).
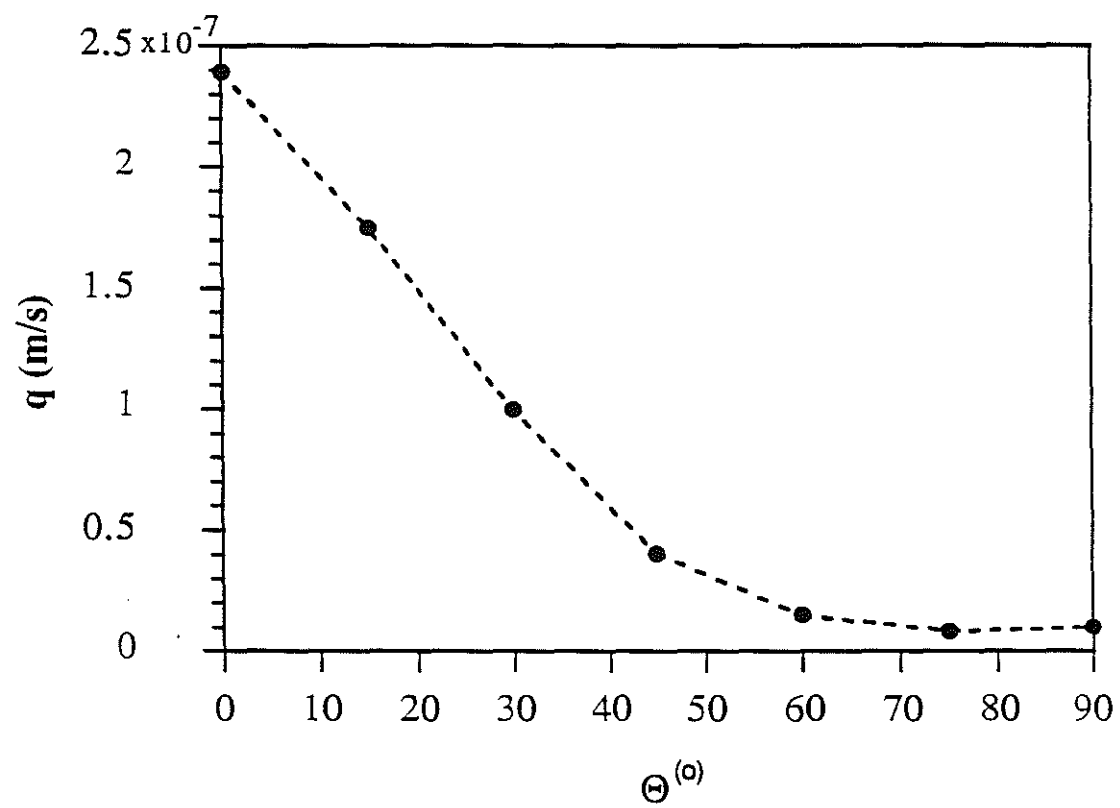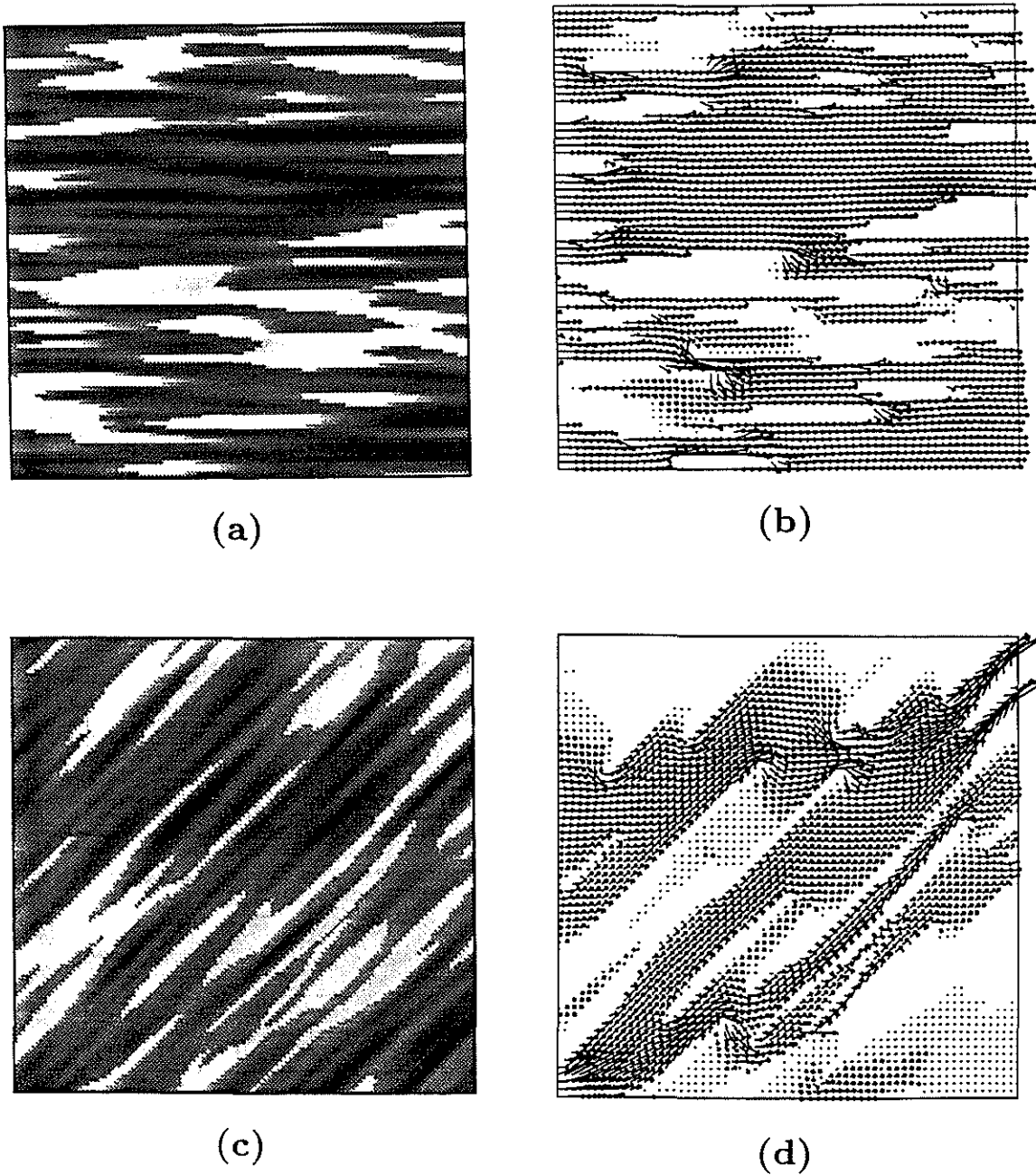
Figure 4: Average flow $\bar{q}$ vs. θ for the case of Figure 6. In the case of aligned fractures, $\bar{k}$ can have an order of magnitude difference between $\theta = 0°$ and $\theta = 90°$, resulting in significant anisotropy (about 184%).
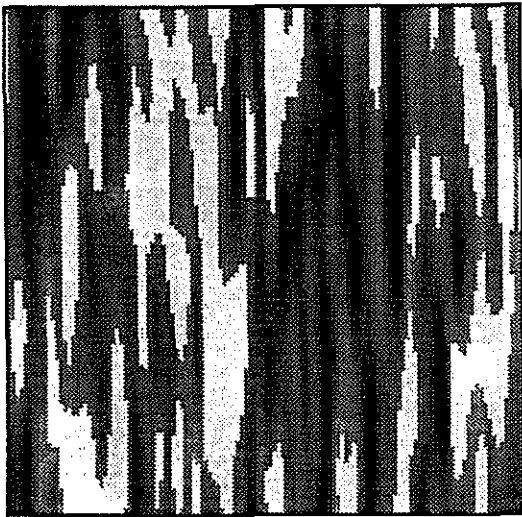
(a)

(b)

(c)

(d)

Figure 5: (a), (c), and (e): aligned barriers distributions with $\theta = 0°$, $45°$, and $90°$. The correlation lengths and model lengths are the same as in Figure 3. (b), (d), and (f): calculated flow fields for $\theta = 0°$, $45°$, and $90°$.
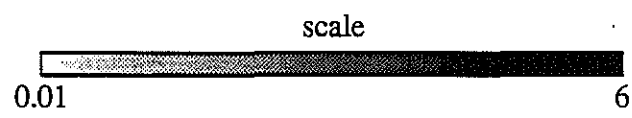
Zhao and Toksöz

(e)   (f)

scale

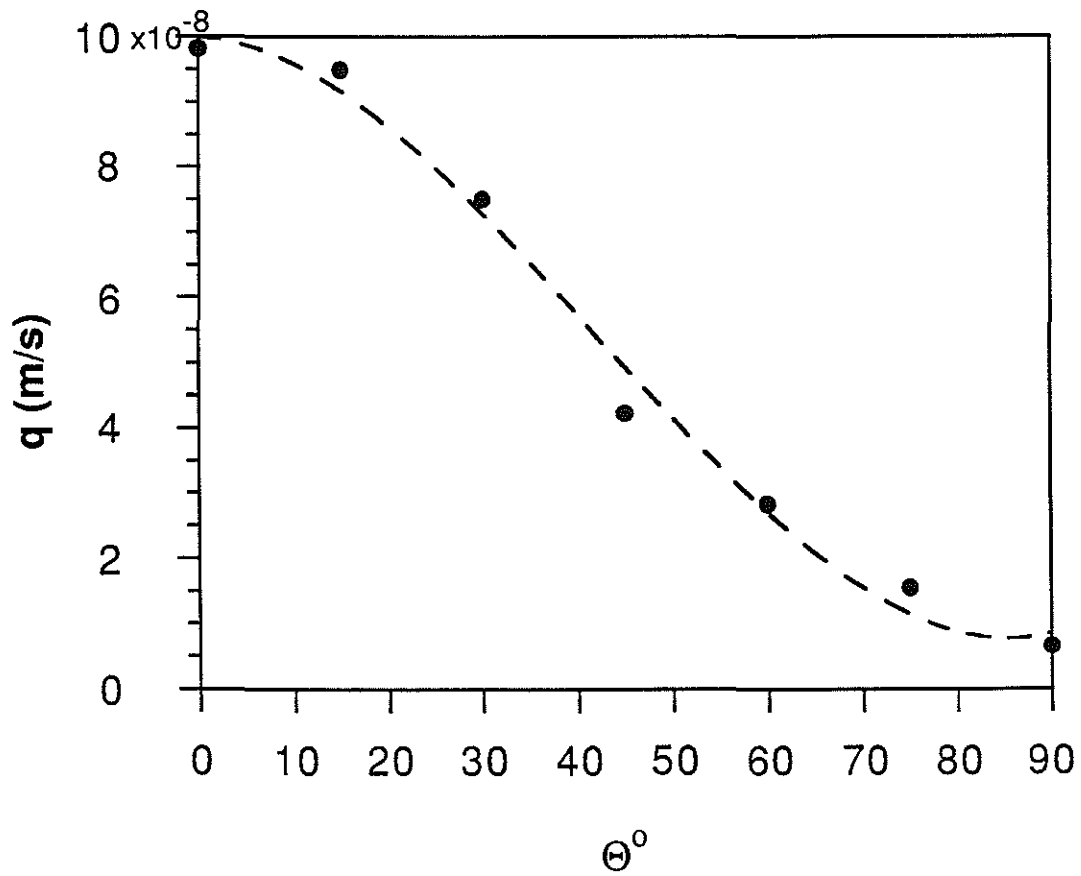0.01   6

Figure 5: continued.

Figure 6: Average flow $\bar{q}$ vs. θ for the case of Figure 5. The permeability anisotropy in this case is about 175%.
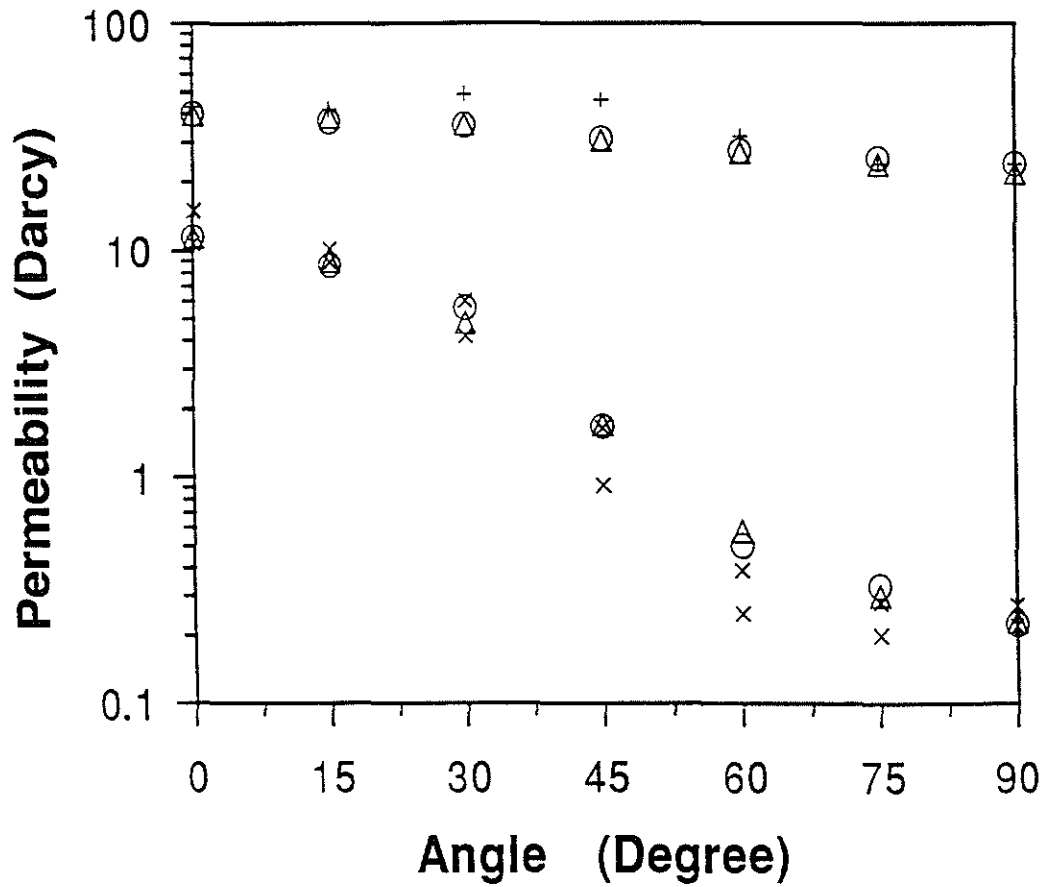
Figure 7: Theoretical (triangles and circles) and experimental (crosses + and ×) results for the two synthetic materials ($k_{90}/k_0 = 0.6$ and $k_{90}/k_0 = 0.02$). Triangles are the anisotropic finite difference modeling results obtained by Bernabé (1991). Circles are the finite difference modeling results of this study.
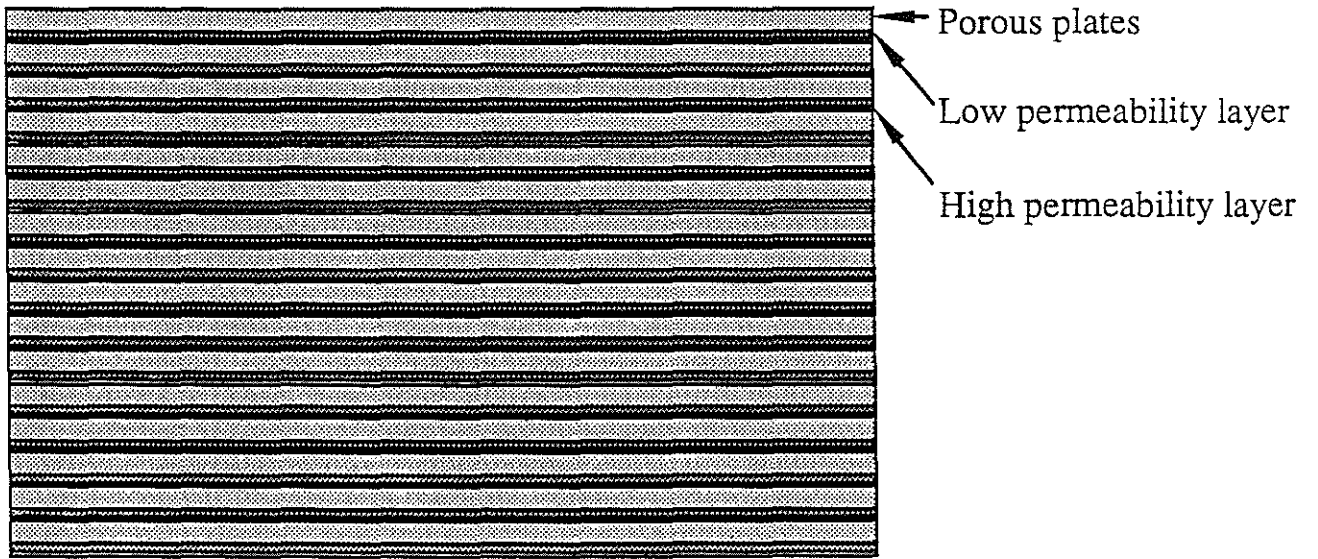
Figure 8: Stacked plates model used in this study.